DURABILITY AND INTERPHASES IN ADHESIVELY BONDED EPOXY-POLYESTER INTERFACES

M. Kanerva[1*], E. Sarlin[2], K. Rämö[2], O. Saarela[1]
[1] Department of Applied Mechanics, Aalto University, Helsinki, Finland,
[2] Department of Materials Science, Tampere University of Technology, Tampere, Finland
* Corresponding author (mikko.kanerva@aalto.fi)

Keywords: *Interface, Adhesive bonding, Pre-treatment, Peel ply*

1 Introduction

1.1 Peel ply surface treatments

Surface treatments for adhesive bonding of composite materials include mechanical abrading, peel plies and a few plasma treatment methods [1,2]. The peel ply surface treatment represents a low-cost and user-friendly method, which can produce an even surface quality for large structures. The challenge in the peel ply treatments is that the success of the bonding on a treated surface tends to be highly material system-specific and a great deal of caution must be placed on the selection of the peel ply product. The reason for the material system-dependence of the peel ply treatment is that a composite material – its matrix above all – interacts chemically with the peel ply. It has been found that the composition of a treated surface depends on the raw material of the peel ply fibres [3]. The exact chemical interaction between a commercial resin and the fibre material is a complex phenomenon and the prediction of the resulting surface modification is difficult.

In this study, we aim to prepare durable composite-composite joints pre-treated using a peel ply prior to bonding. For a proper peel ply surface treatment, the formation of the bond line – i.e. the interface region – is two-fold. First, the peel ply interacts chemically with the composite material during lamination and modifies the surface within removal. Second, the adhesive or overlamination resin interacts with the treated surface. We study typical dry peel plies and a tear ply, which is pre-impregnated by an epoxy resin. Tear plies offer potential for interphase formation, in terms of mixture between two different resin systems: the composite's matrix resin and the tear ply's impregnation resin [4]. We also study a woven stainless steel mesh resembling a 'peel ply' with a minimum polymeric modification on a treated surface; we apply the steel mesh on composites with both epoxy and polyester matrix resins.

1.2 Unsaturated polyester-resin composites

Our study mainly focuses on unsaturated polyester (UP) and glass-fibre based composite materials. In general, polyester matrix-based composites are being used in varied products of infrastructure and marine technology [5,6,7]. The products are typically manufactured by manual lay-up techniques and the surfaces are mechanically abraded in the case of adhesive bonding. Therefore, a question may be raised whether the advantages of the peel ply treatments could be realized in these products.

2 Raw materials and methods

2.1 Laminate preparation

Two different types of laminates were manufactured for further test specimen preparation. Two dis-similar surface treatment techniques were applied: mechanical abrading (grade P36 grit) and peel ply treatments. For the peel ply treatments, four different peel ply products were studied: a polyamide peel ply (A100PS, Richmond Aerovac), a polyester peel ply (Release ply F, Airtech), an epoxy-impregnated tear ply (M21/48%/F08111, Hexcel) and a stainless steel mesh woven of 50 µm diameter AISI 304 strands. For the epoxy-impregnated tear ply, two different procedures were studied: a 5-hour intermediate cure phase at 140 ºC prior to bonding and a continuous room temperature application to longer maintaining a low degree of cure of the impregnation resin.

2.1.1 Glass-UP laminates

The peel ply treatments were mainly studied for a glass-polyester composite. Two different glass-fibre reinforcements were applied: a unidirectional E-glass fibre (EDR-17, Jushi Group) and a chopped strand mat (M501, Ahlstrom). The matrix polymer was an orthophtalic-acid based unsaturated polyester resin (Aropol M 105 TBR, Ashland) cured using a peroxide initiator (Norpol Peroxide 13, Reichold) with a 1.1 % (mass/mass) mixing ratio. Specifically,

the interface between a unidirectional fibre-layer and a strand mat fibre-layer was of interest.

The composites were hand-laminated and cured in ambient laboratory conditions, excluding the intermediate oven-cure phase for studying the use of the epoxy-impregnated tear ply. For the substrate laminates that were peel ply-treated, the peel ply was removed prior to bonding. The 'bonding' refers to *overlamination* of the second adherent on top of the treated substrate laminate. In order to cut wedge and double-cantilevered beam specimens (see section 2.2.3 for details) of the bonded laminates, a pre-crack was prepared by adding a polyamide film (film thickness 50 μm) prior to the overlamination. The pre-crack tip was made sharper by applying a streak of soft graphite-lead pencil (Graphite Pure 2900 3B, Faber-Castell) at the film edge region on the surface of the substrate laminate. When preparing single-lap shear specimens, the lap edges were molded using elastomeric shim pieces in order to avoid unequal fillet effect. The radius of the rounded lap edge corner was approximately 1.2 mm. Details of the single-lap shear specimen preparation were reported in our previous study [4].

2.1.2 Glass-epoxy laminates

In addition to the glass-UP composites, we studied the use of stainless steel mesh surface treatment on glass-epoxy composites with glued bond lines. For this, we used a 0/90° woven glass fabric (3063, 280 g/m^2, Porcher) as a reinforcement. The matrix was of a low-viscosity epoxy-phenol novolak resin (Araldite LY 5052, Huntsman). The epoxy-based resin was cured using a polyamine co-reactant (Aradur 5052, Huntsman) with a 38 % (mass/mass) mixing ratio. The laminates were vacuum injected and cured at ambient laboratory conditions, resulting in an adherent thickness of 3.4 mm. When preparing single-lap shear specimens of these laminates, the adherents were bonded together using a room temperature-curing, rubber-toughened epoxy paste adhesive (DP 190, Scotch-Weld). The bond line thickness was adjusted to 0.9 mm using plastic shimming plates during bonding.

2.2 Mechanical testing

All mechanical tests and related test specimens of this study are listed in Table 1 for convenience.

2.2.1 Single-lap shear testing

Single-lap shear testing, according to the ASTM D5868 standard, was used to study the static strength of the interfaces in ambient laboratory conditions and without any aging treatments for the test specimens. Prior to testing, all the test specimens were post-cured twice at 50 °C for 24 hours using an air-circulating oven. The load rate during the testing was 13 mm/min and nominal width of the specimens was 25.4 mm.

2.2.2 Wedge testing

Wedge testing, according to the ASTM D3762 standard, was used to study the durability of the peel ply pre-treated joints. Prior to aging conditioning, all the test specimens were post-cured twice at 50 °C for 24 hours using an air-circulating oven. The nominal width of the specimens was 25.4 mm and the pre-crack length was 12.5 mm. Before inserting stainless steel wedges (thickness 4.8 mm), the specimens were immersed in distilled water for two weeks (water temperature 64 °C, pH 6). The immersion was continued after the wedge insertion, and the progression of the crack was monitored and recorded within pre-set time intervals. In total, we studied a 200-day conditioning period.

2.2.3 Fracture testing

Interface fracture toughness has been found to be sensitive to peel ply surface treatments [7] and, hence, we aimed to study the stainless steel mesh surface treatment in more detail using fracture testing. Moreover, we wanted to study the effect of the absorbed moisture after the conditioning phase (of wedge specimens) on the interface strength. In order to minimize all specimen preparation-induced variation between wedge and fracture testing, we applied a design-of-experiment test method for using the wedge specimens, described in section 2.2.2, for the testing. Similar kind of further testing of wedge specimens was reported by Armstrong [8]. Our aim was to maintain the wedge-induced mode I crack-tip loading during the further testing. Thereby, we designed removable, external load blocks, which could be fixed to the arms of a wedge specimen, after removal of the wedge. The design of the external load blocks is described in Fig. 1. The method was designated as DCB-X (*Double-Cantilevered Beam* specimens with *eXternal* load blocks). The DCB-X specimens were tested as wet, meaning that they were taken out of the immersion medium (distilled water) and the loading was started within 15 minutes. A conditioning water tank with the immersion medium and the test specimens was let to stabilize at room temperature (21.5 °C) 24 hours prior to testing. The actual testing was performed according to the propagation phase of ISO 15024 standard. A load rate of 2 mm/min was

used. We added the marks for monitoring the crack propagation in the specimens just before testing, using a pencil and thin layer of white, acrylic paint.

In order to study the effect of the conditioning, tested on dry specimens, conventional DCB specimens were prepared. This means that the DCB specimens were conditioned for 140 days submerged in the same immersion medium and temperature with the wedge specimens and, after this conditioning phase, the specimens were let to dry and stabilize in ambient laboratory conditions. During the drying phase, the temperature and air relative humidity were recorded every five minutes, leading to the average values of 22.4 ± 1 ºC and 16.4 ± 5 %RH over the two-month drying period. Prior to the conditioning, i.e., the water immersion, all the test specimens were post-cured twice at 50 °C for 24 hours using an air-circulating oven. The actual testing was performed according to the ISO 15024 standard. Aluminum load blocks were adhesively bonded to nominally 20 mm wide glass-UP specimens with 60 mm long pre-cracks. A load rate of 2 mm/min was applied during the initiation and propagation phases. The testing was performed using a materials testing machine (5967, Instron, USA).

The fracture toughness of the DCB and DCB-X specimens was calculated using the so-called *Corrected Beam Theory*, viz., the following equation [9]:

$$G_I = 3P\delta / (2b[a+\Delta]) \cdot F / N \qquad (1)$$

where P is the load, δ is the load line displacement, b is the width of the specimen, a is the momentary crack length, Δ is the crack length correction term, F is the large-displacement correction factor and N is the load block correction factor. For precise definitions of Δ, F and N, see either the ISO 15024 or ASTM D5528 standard. Only the propagation fracture toughness, G_{Ip}, was determined for the DCB-X specimens, since they had been fractured prior to toughness testing during the wedge testing. For the conventional DCB specimens, the initiation fracture toughness, G_{Ic}, was determined by visual observation of crack onset (i.e., VIS [9]).

2.3 Degree of cure analysis for the tear ply (DSC)

The laminates were cured at ambient laboratory conditions, although the tear ply required elevated temperature curing. Thereby, the degree of cure of the epoxy-impregnated tear ply was studied using a differential scanning calorimeter (DSC 204 F1, Netzsch, Germany). The analyses covered a typical heating rate of 10 °C/min and a temperature range of 25…300 °C according to a typical DSC procedure. Special attention was given to the sample preparation in order to prevent unwanted curing during transportation; the samples were analyzed within three hours and transported to the instrument at a temperature below –10 °C using a thermally insulated carrier.

2.4 Microscopic analysis (FESEM)

The peel ply fibres, laminate fracture surfaces and interfaces were studied using a field-emission scanning electron microscope (ULTRAplus, Zeiss, Germany). Special attention was given to the sample preparation in order to avoid surface charging and effect of polishing pastes or solvents. Whenever it was observed sufficient, a thin, evaporated carbon coating was used to enable conductivity on the polymeric samples. Otherwise, a thin gold coating was applied.

2.5 Compositional analysis (EDS)

Compositional analysis is a pre-requisite for a peel ply study because unwanted residues from peel ply fibres with a possible release finish can contaminate the composite surface during the treatment [10]. We applied X-ray energy dispersive spectroscopy (INCA Energy 350, Oxford Instruments, UK) in order to determine elemental compositions of different samples. Additionally, EDS was used to investigate the interphase structure of the bonded laminates, for which the bond surfaces had been treated using the epoxy-impregnated tear ply. For this, we used a line-scan analysis to map discrete spatial distributions of the (detectable) elements. A cross-sectional sample was prepared for the line-scan using ultramicrotomy. Only a thin, evaporated carbon coating was applied on the EDS samples prior to the analysis.

3 Results

3.1 Shear strength of joints

The shear strength screening tests of the specimens with different surface treatments showed that the mechanical abrading, the polyamide peel ply and the tear ply with the continuous room temperature application resulted in full, 100 % cohesive failure in the adherent composites for all the tested specimens. In contrast, the fracture surfaces of the specimens pre-treated using the polyester peel ply showed some

adhesive failure-regions, that is, the use of the polyester peel ply was seen unreliable. Even worse, the treatment with the tear ply with an intermediate cure prior to bonding resulted in full adhesive failure. More details of the testing and the analysis of the screening were reported in our previous study [4].

The surface treatment with the stainless steel mesh on the *glass-UP* composite resulted in fully cohesive failure in the adherent composites for all the specimens: the test series manufactured using exactly the same resin-catalyst mixture gave the shear strength values of 5.0 ± 0.3 MPa and 6.5 ± 0.4 MPa, for the stainless steel mesh and mechanical abrading treatment, respectively. The values are based on a minimum of five specimens. The treatment with the stainless steel mesh on the *glass-epoxy* composite resulted in fully cohesive failure in all the specimens – similarly as for the glass-UP composite. The test series manufactured using exactly the same resin-co-reactant mixture and the same adhesive gave the shear strength values of 14.2 ± 0.3 MPa and 13.9 ± 0.4 MPa, for the stainless steel mesh and mechanical abrading treatment, respectively. The values are based on six specimens for the abrading and three specimens for the stainless steel mesh. The higher values for the glass-epoxy specimens (when compared to glass-UP) are mostly due to the higher strength of the epoxy polymer. Because the failure mode was fully cohesive for the both composite systems, the shear strength values merely correspond to the mechanical performance of the composite / adhesive.

3.2 Interface durability

The surface treatments, which resulted in a fully cohesive failure during the quasi-static testing in ambient laboratory conditions, were selected for the wedge testing. The crack lengths in the specimens with a wedge inserted, as a function of time during the water immersion, are shown in Fig. 2. Each curve represents the average behavior of five specimens. The flatness of the crack length versus time -curves in Fig. 2 (a) indicates that all of the joints were rather durable against the elevated temperature water immersion. In other words, the crack progression through the entire period was very low or non-existent after the first 16 hours with wedges inserted. However, it should be noted that the crack-tip loading due to the wedge decreases for an increasing crack length and, thus, the exertion was not equal in different specimens. For example, it is possible that there would have been continuous, non-negligible crack growth at a higher loading in the joints pre-treated using the epoxy-impregnated tear ply with a continuous room temperature application, which resulted in the longest cracks immediately after the wedge insertion, and consequently in a very low crack-tip loading for the rest of the conditioning period.

It can be seen that the fracture resistance of the joints pre-treated using either the mechanical abrading or stainless steel mesh was least affected by the two-week pre-immersion; the total crack length immediately after the wedge insertion (time = 0 h, Fig. 2 (b)) was low (58.1 ± 1 mm and 60.2 ± 2 mm). In comparison, the crack length was considerably (78.4 ± 13 mm and 84.6 ± 10 mm) higher, for the polyamide peel ply and the epoxy-impregnated tear ply treatment with the continuous room temperature application.

3.3 Interface fracture toughness

G_{Ip} value for the DCB-X specimens, tested as wet, was 797.6 ± 164 J/m^2. The value is based on five specimens. The failure mode during the DCB-X testing was cohesive in the adherent composites for all the specimens. G_{Ic} value for the DCB specimens, tested in dry condition, was 380.4 ± 68 J/m^2. G_{Ip} value for the DCB specimens, tested in dry condition, was 884.6 ± 205 J/m^2. The values are based on five specimens. Similarly as for the DCB-X, the failure mode during the DCB testing of dried specimens was cohesive in the adherent composites for all the specimens, as shown in Fig. 3 (a).

The fact that all the fracture test specimens failed fully cohesively proves that the stainless steel mesh treatment gave durable composite-composite joints, which endured long-term water immersion at an elevated temperature. A comparison of the DCB-X and DCB fracture toughness values suggests that the effect of absorbed moisture was low or insignificant on the (residual) fracture toughness of the long-term conditioned glass-UP composite laminates. The low value of the initiation fracture toughness (when compared to the propagation toughness) indicates that the pre-crack tip was very sharp and enabled crack initiation at a low crack tip loading. The absolute fracture toughness values are high when compared to corresponding values found in the literature for similar materials [7,11] – this might be due to the strong fibre-bridging that occurred during the fracture here.

3.4 Intermediate cure for tear ply treatment

DSC curves for the epoxy-impregnated tear ply are shown in Fig. 4. For a sample measured at a representative b-stage, i.e., after taking it out from a freezer, there is a clear exothermic peak that corresponds to the cure of the impregnation resin. For a sample with a cure at 140 °C for five hours (resembling the intermediate cure within a tear ply treatment for a laminate), the exothermic peak has almost disappeared, meaning that the 5-hour cure at 140 °C led to essentially full degree of cure of the impregnation resin (calculated degree of cure ≈96 % relative to the b-stage heat of cure).

An advantageous effect of a low degree of cure of the adherent laminate has been reported for carbon-fibre and epoxy composites bonded with an adhesive [12]. In our study, to form a tough interphase between the tear ply-modified surface and the polyester overlamination resin, a proper amount of polymer interpenetration is presumably needed. We consider that a low degree of cure of the tear ply (its impregnation resin) could enable some level of interdiffusion or interpenetration between the impregnation resin and the unsaturated polyester resin of the composite. It has been found that epoxy-polyester mixtures with a correct stoichiometry can form mechanically tough, interpenetrated phases [13]. It should be noted that when a composite laminate with unsaturated polyester matrix resin is treated using the tear ply, the curing process of the impregnation resin might change. Lin et al. [13,14] have studied the cure kinetics of polyester-epoxy mixtures and observed that the polyester resin can have a catalytic effect on the epoxy curing. Therefore, further studies are needed for understanding the curing of the actual laminate *surface* and the treatment using a tear ply.

3.5 Interface structure

First, we studied the surface composition of the peel ply products and the results are shown in Table 2. It can be seen that there was no fluorine (F) or reliable silicon (Si) content found on the peel ply fabrics. Based on the results, the peel plies were considered free of fluorine and silicon-containing surface finishes and, respectively, the interfaces in the bonded laminates were free of contamination.

The sharpness of the pre-cracks at interfaces was studied by cutting cross-sectional samples from the pre-crack tip region in bonded laminates. Fig. 3 (b) shows that there might have been two potential sites for the initiation. First, the graphite residue from the lead pencil formed thin seams, which could have worked as a pre-crack tip. Second, the interface – modified by the peel / tear ply treatment – tended to involve local debonding on a micro scale and a coalescence of these debonds could have been worked as a pre-crack tip. Coalescence can be due to handling of the laminates, such as the cutting of the specimens, which perhaps induced slight peeling load at the region of the polyamide film tip. A detailed study, as shown in Fig. 5 (a), shows FESEM imaging of the interface region of a glass-UP bonded laminate pre-treated using the tear ply and the continuous room temperature application. It can be seen that micro-scale debonding occurred at the peel ply fibre-moulded cavities already before any mechanical testing. The debonding can be, in part, the result of traditional sample preparation by a polishing procedure, which was applied to the cross-sectional sample. Anyhow, it is clear that the fibre-moulded cavities are the weakest point for the tear ply pre-treated specimens in our study. In general, we consider that the shape of the cavities might emphasize the cure-shrinkage induced stresses at interface, as described schematically in Fig. 5 (b). The shrinkage, combined with presumably poor adhesion at the cavities, would definitely lower the interface strength when peel plies have been applied.

The results of the line-scan analysis are shown for nitrogen (N) and oxygen (O) relative to carbon (C) concentration, in Fig. 6. The interface sample for the line-scan was cut off a glass-UP bonded laminate pre-treated using the tear ply with the continuous room temperature application. It seems that the determination of an interphase region according to pure elemental contents is challenging. The nitrogen traces found (and assumed to derive from poly-amine co-reactants of the impregnation resin) were distributed over a considerably wide range when compared to the potential impregnation resin left on the surface. Anyhow, the tear ply treatment left the treated, unbonded composite surface with a layer of impregnation-resin and, an epoxy-UP interphase might have formed during the bonding depending on the interaction between the two resin systems. The transfer of the impregnation resin was studied via optical imaging of the tear ply removed from a laminate surface within the treatment, as shown in Fig. 7. Comparison to FESEM imaging of cured, bare tear ply samples [4] showed that approximately a half of the impregnated resin (20…70 µm thick layer) tends to be left on the laminate surface.

3.6 Stainless steel mesh-treated laminate surface

In principle, the stainless steel mesh surface treatment works similarly to any polymeric peel ply treatment. The steel mesh got fully wetted by the composite resin (Fig. 8 (a)) and left the surface with a specific texture based on the mesh weaving, as shown in Figs. 9 (a) and 9 (b). On the other hand, the stainless steel mesh had relatively large open spaces between the individual strands when compared to, for example, the polyamide peel ply, which consists of fibre bundles, as shown in Fig. 8 (b). The open spaces resulted in regions of fractured matrix when the mesh was being ripped off. The stainless steel strand diameter is also twice as large (50 μm) when compared to an individual polyamide fibre (25 μm).

The very good mechanical performance of the composite interfaces pre-treated by the stainless steel mesh might be due to multiple factors. First of all, the large amount of open spaces in the steel mesh resulted in a large surface area of fractured matrix on the treated composite surface. The fractured regions in general are regarded as clean and fresh sites for successful bonding. Second, it is unlikely that the stainless steel could significantly interact with the composite's matrix resin. The stainless steel mesh treatment resulted in a similar failure mode when applied to epoxy and UP resin composites, which could – at maximum – indicate a similar interaction between the mesh and either of the two resins. We doubt any interaction. Third, it is clear that a metallic mesh is not able to leave any polymeric residue (from itself) on a surface, in contrast to polyamide and polyester peel plies. Therefore, we presume that the stainless steel strand-molded cavities essentially represented the composite's matrix resin composition. In theory, a stainless steel strand could transfer a part of its surface oxide layer, metal elements or residues from a mesh cleaning procedure onto a treated laminate surface. An initial analysis of the elemental composition of the stainless steel mesh-treated surface (using EDS) did not indicate an observable amount of metals that could have transferred onto the laminate. To verify the non-existence of metal, more surface sensitive methods will be attempted.

4 Conclusions

The use of polymeric peel plies, meaning a polyester, polyamide and an epoxy-impregnated tear ply, led to a low durability in our overlaminated glass-UP composites-composite joints, which were immersed in 64 °C water for an extended period. In contrast, the application of mechanical abrading or a stainless steel mesh resulted in durable and crack resistant joints with fully cohesive failure in the adherent composites upon mechanical testing. The finding suggests that a polymeric peel ply might modify the composite surface within its removal and, consequently, durable bonds cannot form on the composite surfaces when being overlaminated. However, the interaction between the composite's matrix resin and peel ply fibres – or the impregnation resin of a tear ply – must be highly material system-dependent and more detailed studies are needed in order to understand the contribution of pure bulk composite aging to the interface region's degradation due to water immersion at an elevated temperature.

The surface treatment using a tear ply with a continuous room temperature application did not assure high durability in our study. Investigations of the cross-sectional interface region in overlaminated joints revealed that local micro-scale debonding occurred along the cavities, which formed prior to bonding within the tear ply's removal. The cavities were molded by individual peel / tear ply fibres and represented potential crack initiation sites. A study of the elemental composition at the interface region showed that determining an interphase is not straightforward for a composite with a commercial resin, fibres and a tear ply product. Therefore, subsequent, repeated analyses, at minimum, are important in the future work.

The surface treatment using a stainless steel mesh on the composite substrate laminate resulted in as strong and durable composite-composite joints as the mechanical abrading. This result confirmed the conception that treated surfaces with the minimum 'polymeric' modification are most suitable for adhesive bonding. The fracture toughness of the long-term aged glass-UP composites was high and, respectively, the interface was even stronger – forcing the crack to deflect from sharp pre-cracks towards the bulk composite and induce fibre-bridging.

Acknowledgement

The presented study was funded by Finnish Metals and Engineering Competence Cluster (FIMECC) and a grant by Graduate School of Mechanics of Materials.

References

[1] M. Kanerva, O. Saarela "The peel ply surface treatment for adhesive bonding of composites: a review". Int J Adhes Adhes, Vol. 43, No. 1, pp 60-69, 2013.

[2] G. Wachinger et al. "New trends in CFRP treatment and surface monitoring for automated structural adhesive bonding". *Proceedings of the international conference on composite materials*, Edinburgh, UK, 2009.

[3] Q. Bénard, M. Fois, M. Grisel "Peel ply surface treatment for composite assemblies: chemistry and morphology effects". Compos A, Vol. 36, No. 11, pp 1562-1568, 2005.

[4] M. Kanerva, E. Sarlin, K. Rämö, O. Saarela "Interface modification of glass fibre-polyester composite-composite joints using peel plies". Sent for acceptance, 2012.

[5] P. Ziehl, T. Fowler "Fiber reinforced vessel design with a damage criterion approach". Compos Struct, Vol. 61, No. 4, pp 1-17, 2003.

[6] G. Di Bella, L. Calabrese, C. Borsellino "Mechanical characterisation of a glass/polyester sandwich structure for marine applications". Mat Des, Vol. 42, No. 1, pp 486-94, 2012.

[7] P. Davies, C. Baley, H. Loaec, Y. Grohens "Interlaminar tests for marine applications. Evaluation of the influence of peel plies and fabrication delays". Appl Compos Mat, Vol. 12, No. 5, pp 293-307, 2005.

[8] K.B. Armstrong "Effect of absorbed water in CFRP composites on adhesive bonding". Int J Adhes Adhes, Vol. 16, No. 1, pp 21-28, 1996.

[9] Fibre-reinforced plastic composites – determination of mode I interlaminar fracture toughness, G_{Ic}, for unidirectionally reinforced materials. ISO 15024 International Standard, 2001.

[10] L.J. Hart-Smith, G. Redmond, M.J. Davis "The curse of the nylon peel ply". Tech Rep, MDC 95K0072, McDonnell Douglas, 1996.

[11] Y. Perrot, P. Davies, A. Kerboul, C. Baley "Marine composites based on low styrene content resins. Influence of lamination procedure and peel plies on interlaminar resistance". Appl Compos Mat, Vol. 15, No. 2, pp 87-97, 2008.

[12] B. Flinn, J. Satterwhite, J. Aubin "Effect of laminate cure conditions on bond quality of peel ply prepared surfaces". *Proceedings of the international SAMPE symposium and exhibition*, Baltimore, USA, 2009.

[13] M-S. Lin, C-C. Liu, C-T. Lee "Toughened interpenetrating polymer network materials based on unsaturated polyester and epoxy". J Appl Polym Sci, Vol. 72, No. 4, pp 585-592, 1999.

[14] M-S. Lin, R-J. Chang "Chemorheology on simultaneous IPN formation of epoxy resin and unsaturated polyester". J Appl Polym Sci, Vol. 46, No. 5, pp 815-827, 1992.

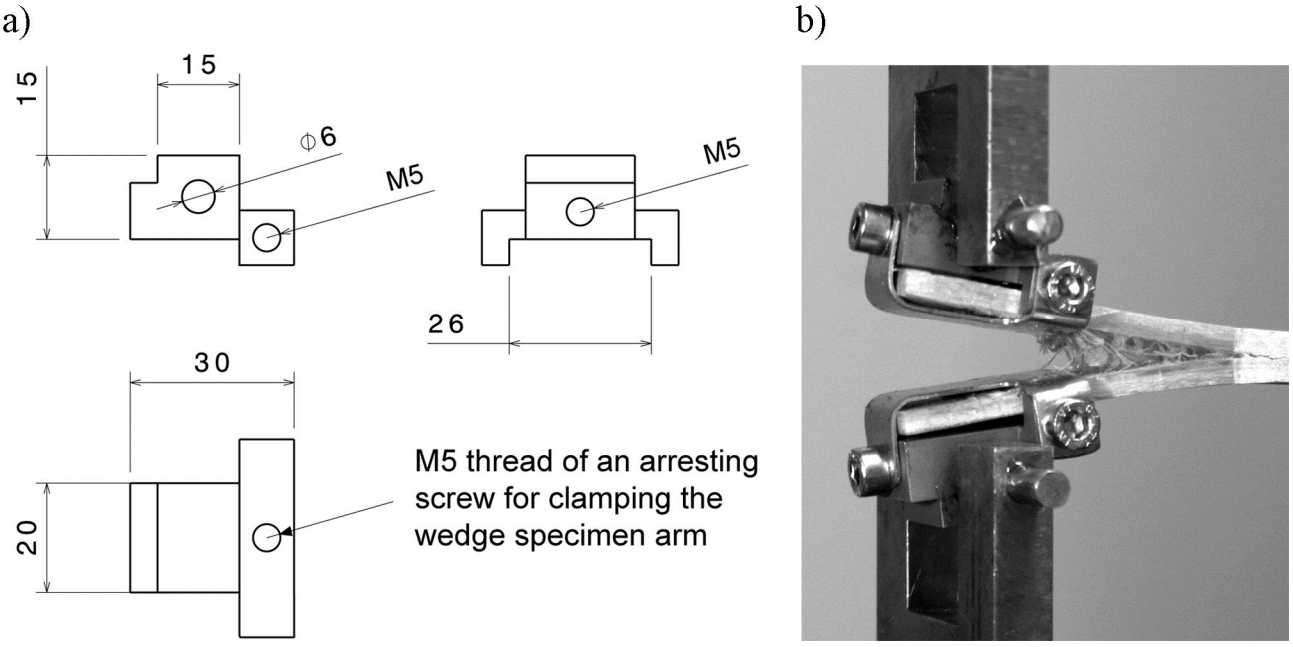

Fig.1. Description of the external load blocks for DCB-X fracture testing: a) main dimensions of an external load block and; b) test setup during DCB-X testing. Dimensions are in millimeters.

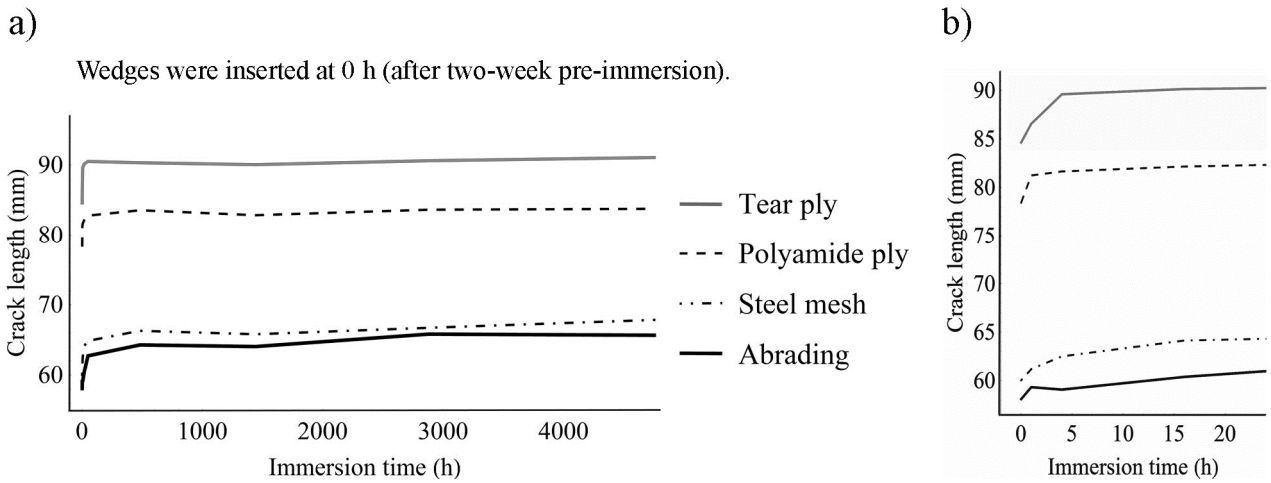

Fig.2. Durability testing of glass-UP composite-composite joints using wedge specimens: a) curves of crack progression through the entire immersion period and; b) detail of the curves that shows initial crack lengths within wedge insertion and the resulting crack progression during the first 24 hours.

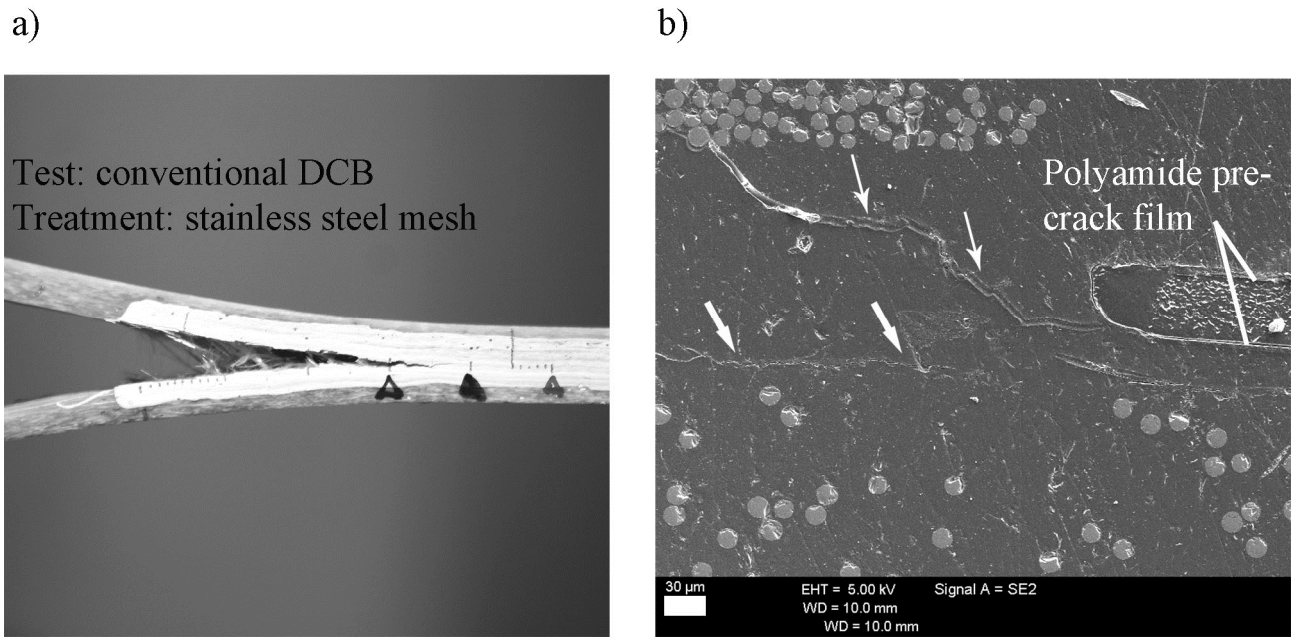

Fig.3. Fracture study of aged DCB specimens: a) cohesive failure and strong fibre-bridging during conventional DCB testing of a glass-UP specimen pre-treated using stainless steel mesh; b) FESEM imaging of the pre-crack tip showing two potential initiation sites – the thin arrows indicate seams of graphite residue from a lead pencil prior to bonding and the thick arrows indicate presumed micro-scale debonding along the interface.

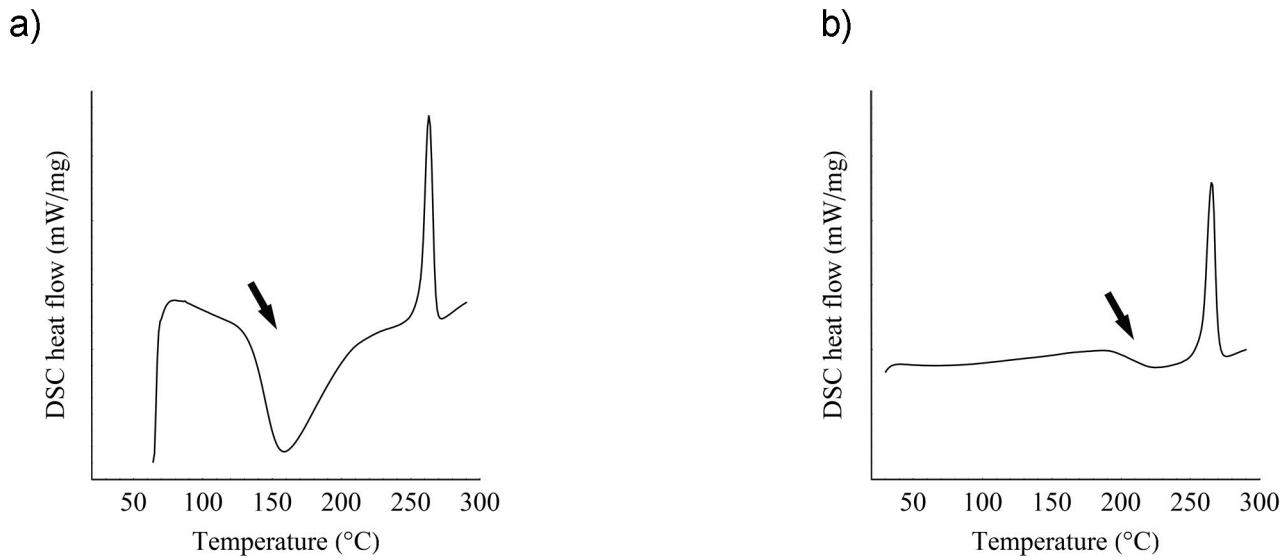

Fig.4. Cure study of the impregnation resin of the tear ply: a) DSC rate profile for a tear ply sample at the b-stage (gelled stage); b) DSC rate profile for a tear ply sample after the 5-hour oven cure (140 ºC). The arrows indicate the exothermic peaks related to curing reactions.

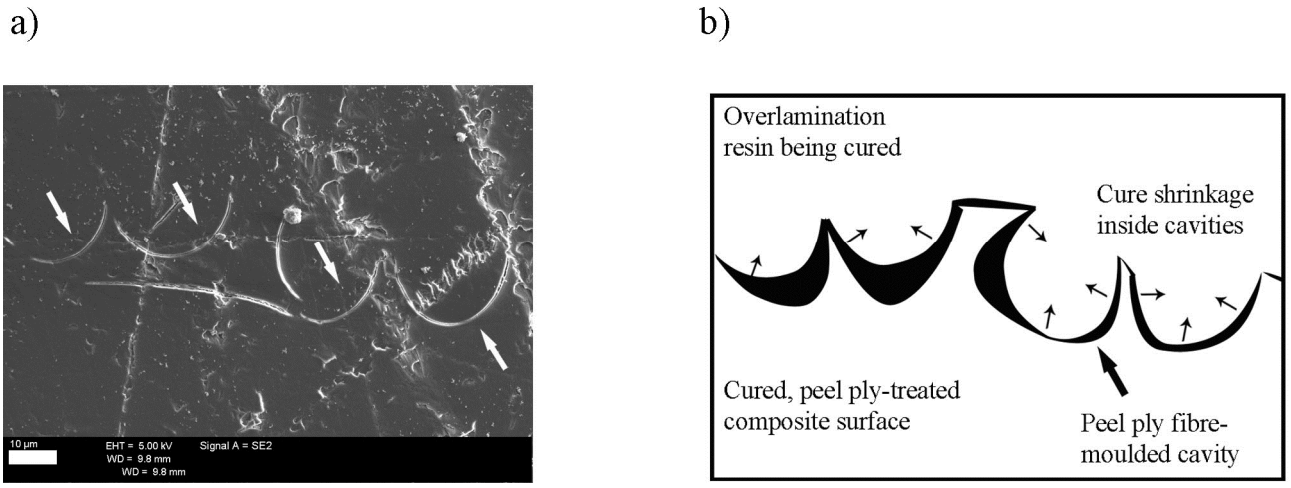

Fig.5. Cross-sectional FESEM imaging of a bonded laminate interface: a) local, micro-scale debonding at peel ply fibre-moulded cavities and; b) schematic illustration of cure shrinkage-induced peeling at fibre-moulded cavities.

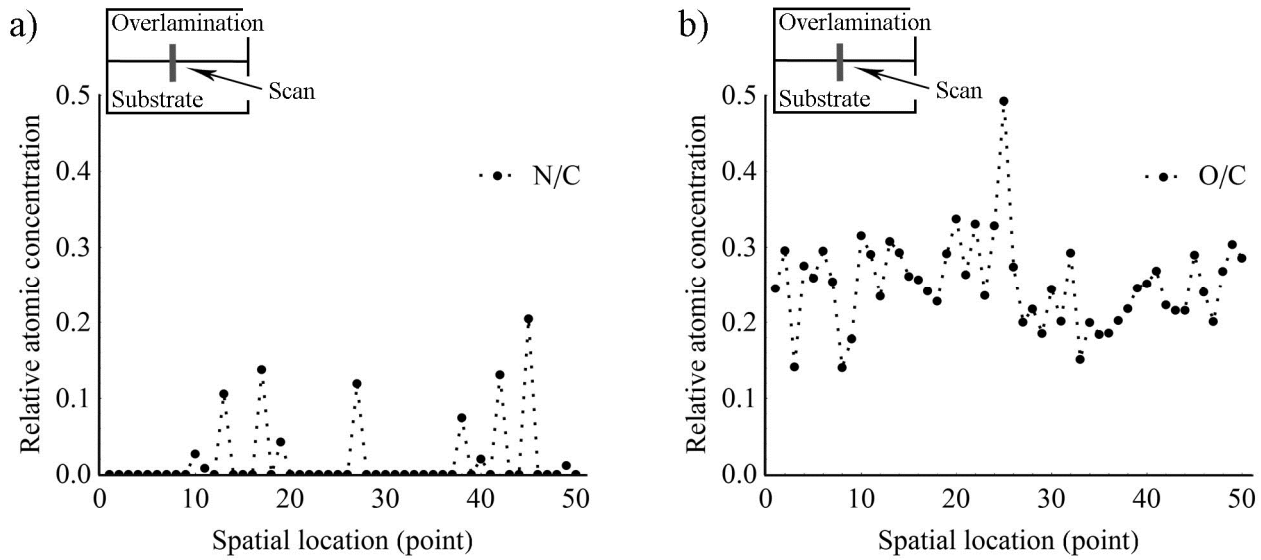

Fig.6. Compositional analysis using a line-scan cross the interface region (total scan length 950 μm): a) carbon-relative concentration of nitrogen and; b) carbon-relative concentration of oxygen.

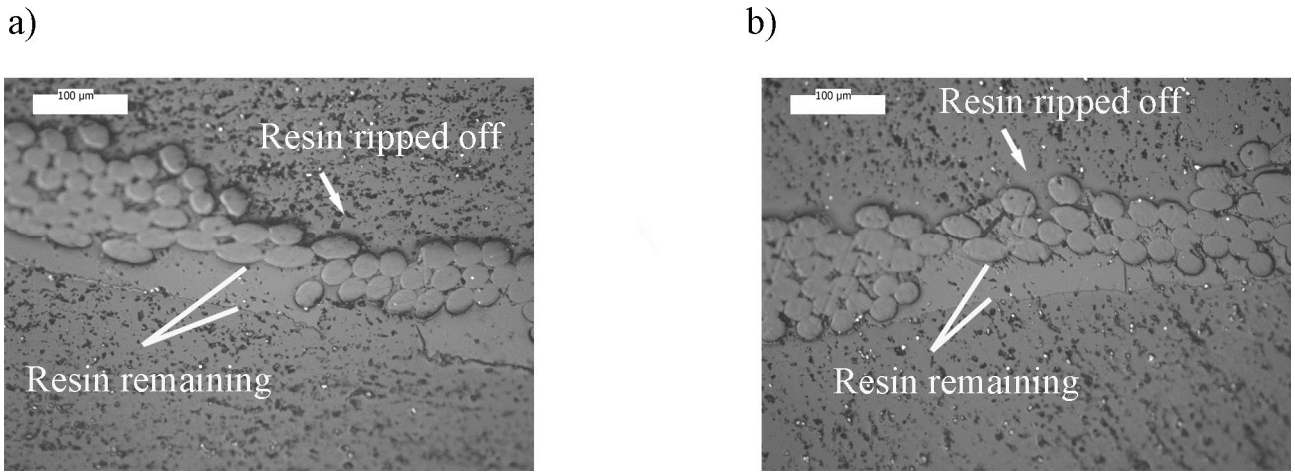

Fig.7. Optical microscopy imaging of tear ply sheets after removal from composite surface: a) cross-section of a tear ply sample removed from the composite surface after the 5-hour intermediate oven cure (140 ºC) and; b) cross-section of a tear ply sample removed from the composite surface after the continuous room temperature application. When compared to a bare tear ply, half of the impregnation resin was estimated being transferred to a treated composite surface.

a) b)

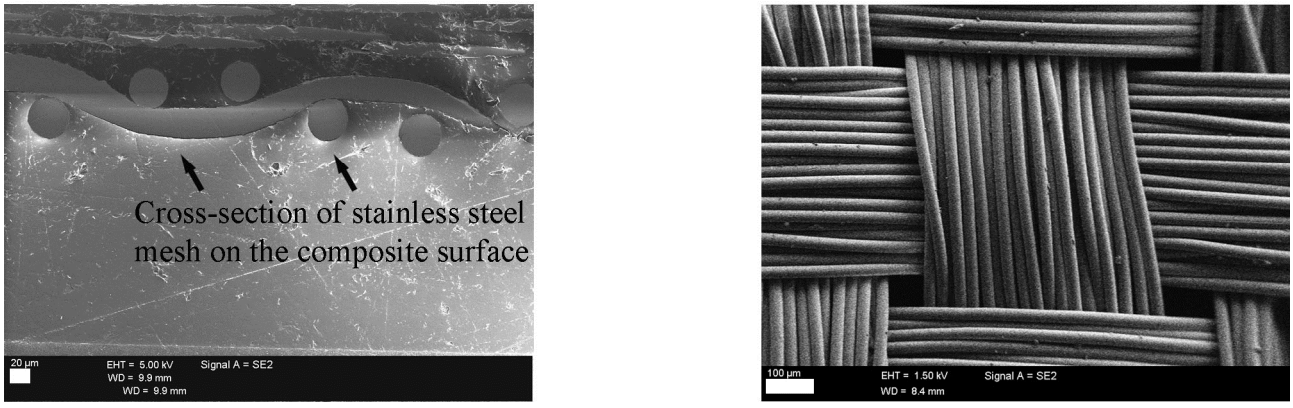

Fig.8. FESEM imaging of the stainless steel mesh and polyamide peel ply: a) cross-section of stainless steel mesh on glass-UP composite surface as a surface treatment ply and; b) FESEM imaging of polyamide fibre bundles in the peel ply fabric. Note different scale bars.

a) b)

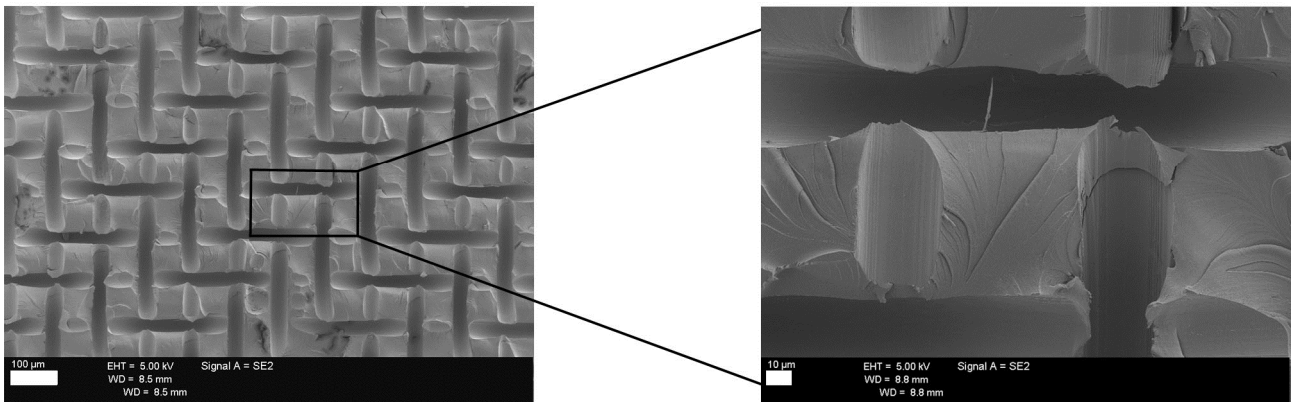

Fig.9. FESEM imaging of the stainless steel mesh-treated glass-UP composite surface: a) general view of the texture and; b) detail of fractured matrix and stainless steel strand-molded cavities.
Note different scale bars.

Table.1. Performed tests, material data of test specimens and the surface treatments prior to bonding.

Conducted mechanical tests per composite material and surface treatment prior to bonding	Single-lap shear ASTM D5868	Wedge ASTM D3762	DCB-X	DCB ISO 15024
Glass-UP (mechanical abrading)	✓	✓	-	-
Glass-UP (polyester)	✓	-	-	-
Glass-UP (polyamide)	✓	✓	-	-
Glass-UP (tear ply, intermediate cure)	✓	-	-	-
Glass-UP (tear ply, room temperature application)	✓	✓	-	-
Glass-UP (stainless steel mesh)	✓	✓	✓	✓
Glass-epoxy (stainless steel mesh, epoxy adhesive)	✓	-	-	-

Table.2. Elemental contents of dry peel ply fabrics according to EDS analysis.

Composition [in At%]	C	N	O	Si	F
Polyamide peel ply	66	16	18	< 1	-
Polyester peel ply	67	-	33	< 1	-